EFFICIENT NUMERICAL METHODS FOR AEROELASTIC ANALYSIS OF WING-PROPELLER CONFIGURATION COMPOUND HELICOPTERS

Zi Wang[1*], Alessandro Anobile[1], Atanas A. Popov[1]

[1] Department of Mechanical, Materials and Manufacturing Engineering, University of Nottingham, University Park, Nottingham, UK

*eaxzw2@nottingham.ac.uk

ABSTRACT

Efficient numerical methods for time-domain aeroelastic analysis of a wing structure under a propeller-wing configuration is described in the paper. A linear beam model with deformable elastic axis under torsion and flapping is considered to simulate a wing structure with a tip-mounted propeller, relying on efficient, analytical formulations. The complete aeroelastic system of equations is then solved using Galerkin's approach, and numerically integrated by the Newmark-beta method. The computational tool developed is able to efficiently predict in the time domain the wing aeroelastic transient behaviour and the wing-propeller interaction effects. The purpose of the tool developed is to provide accurate enough predictions of the system aeroelastic response to be included in structural optimisation and control synthesis procedures. A detailed analysis on the solver used and an aeroelastic case study of a Eurocopter X3-like compound helicopter wing/propeller configuration are demonstrated.

Keywords: Aeroelasticity, Compound helicopter, Numerical method

1 INTRODUCTION

The high level of vibration resulting from the fluid-structure interaction is still a major and open issue in rotorcraft design, affecting the fatigue life of structures, maintenance costs, on-board instrumental efficiency and comfort. Compound helicopters, equipped with wings for increased lift in fast forward flights, have additional vibration sources from the propellers located at wing tips and from the presence of power transmission system in the wing structure. Being able to simulate the complex aeroelastic behavior associated with such configuration is extremely important during the design stages.

In this paper, the attention is focused on the numerical efficiency of a computational tool for aeroelastic analysis, particularly suited for optimisation and control synthesis processes. In order to achieve efficiency, the time-domain prediction of aerodynamic loads, due to wing/propeller interaction relies on analytical sectional theories. These theories commonly use convolutional integrals to take into account the aerofoils aerodynamic history. Consequently, a large set of data is needed at each iteration of the numerical process performed, decreasing the numerical efficiency of such simplified approaches.

In the past, numerical studies were carried out to model the unsteady response of elastic wings relying on analytical sectional model. Sears and Sparks [1] studied the effect of a sharp-edged gust on an elastic in bending but torsionally rigid wing using Jones' approximation [2, 3] of the Wagner's function. As performed by Jones for the Wagner's function, a similar exponential expression was proposed for the Küssner's function by Sears and Sparks for its simplicity [1]. In a more recent work, the plunging motion of a typical sectional model under sharp edged gust was further analysed for its flutter boundaries and studied under sev-

eral flutter related conditions by Kargarnovin and Mamandi [4]. Extending the sectional model to include torsional behaviour, aeroelastic analysis under sharp edged gust was carried out by Shams et al. using a recursive approximation for the Wagner's function [5]. Additional studies were carried out by Marzocca et al. that examined the aeroelastic instability and response of 2D aerofoil under arbitrary gust loadings using Wagner's and Küssner's models [6].

Here, a model for aeroelastic analysis of wing-propeller configurations is presented, and different numerical solution strategies implemented and compared. A recursive algorithm has been implemented to overcome the inefficiency brought by convolutional integrals. For the case study analysed, the aircraft wing is simplified as a cantilever beam with its cross-sections considered as aerofoils in the aerodynamic loads calculation. The aerodynamic effect of propeller mounted on the wing is modelled as sinusoidal wake inflow travelling through the wing structure, adding axial and vertical velocity components to the wing surface. Wagner's [7] and Küssner's [8] functions are used to characterise the aerodynamic lift generated on the span with the additional axial and vertical velocity components respectively. The complete aeroelastic model is solved numerically by the Newmark-beta method [9].

2 THEORETICAL BACKGROUND

2.1 Structural Dynamics

Considering the *x*-axis aligned with the wing elastic axis, the governing equations, normalised in dimensionless time-domain, can be obtained considering torsional and flapping (*z*-direction) behaviour as

$$\begin{aligned} \ddot{\xi} + \chi_\alpha \ddot{\alpha} + \frac{c_h b}{m U_\infty}\dot{\xi} + \frac{b^2}{m U_\infty^2}(EI\xi'')'' &= l_h(x,\tau) \\ \ddot{\alpha} + \frac{\chi_\alpha}{r_\alpha^2}\ddot{\xi} + \frac{c_\alpha b}{I_\alpha U_\infty}\dot{\alpha} - \frac{b^2}{I_\alpha U_\infty^2}(GJ\alpha')' &= m_\alpha(x,\tau) \end{aligned} \tag{1}$$

In Eq. (1), ξ, α are the dimensionless bending and torsional displacements, m and I_α are the mass and mass moment of inertia per unit span, respectively, U_∞ is advancing speed of the aircraft, b is the half chord length, χ_α is the dimensionless static unbalance at the shear centre, r_α is the dimensionless radius of gyration, c_h, c_α being the damping coefficient, EI and GJ are the bending and torsional stiffness, respectively, and l_h, m_α are the dimensionless loadings in the corresponding coordinate. Note that $\dot{\xi}\ \ddot{\xi}\ \dot{\alpha}$ and $\ddot{\alpha}$ are dimensionless time differentials with respect to non-dimensional time τ, whereas ξ' and α' are length differentials with respect to *x*-axis. Similar formulations can be found in Reference [10]. Using modal analysis techniques, bending and torsional displacements can be solved with mode shape functions of a cantilever beam. Loadings in bending and torsional coordinate consist of generalised loadings (F_{gen}) and aerodynamic loadings (l_a, l_g, m_a, m_g). In addition to the aerodynamic loads, only the concentrated propeller weight at wingtip ($F_{\text{gen}} = b/mU_\infty^2 \times \text{propeller weight}$) is considered in this case, neglecting effects of forward thrust and rotational moment. Also at this stage, the wing dynamics is not coupled with the propeller dynamics, assuming only the tip-weight on the cantilever beam and the aerodynamic interaction as effects of the propeller presence.

2.2 Aerodynamic Loadings

A fixed-wing with a built-in angle in forward flight is subjected only to a constant advancing speed along the span and a vertical component (simulated as "equivalent step-gust") due to the pre-twist angle and angle of attack. In the application considered, the presence of the propeller affects the wing behaviour by its wake slipstream. As illustrated in Figure 1, the inflow coming from the propeller has two main characteristic velocity components, one being axial

and the other being a vertical component. At this level, the third component, horizontal along the wing span, is neglected. Therefore, the total aerodynamic loadings can be split into different contributions, including: 1) constant advancing flow along wing span, 2) additional step-like advancing flow at the propeller covered area produced by thrust generation, 3) an "equivalent step-gust" $w_0(x,\tau)$ applied along the wing span to model the wing built-in pretwist angle and 4) sinusoidal vertical inflow produced by propeller presence. They can be characterised analytically by relying on sectional aerodynamic theories.

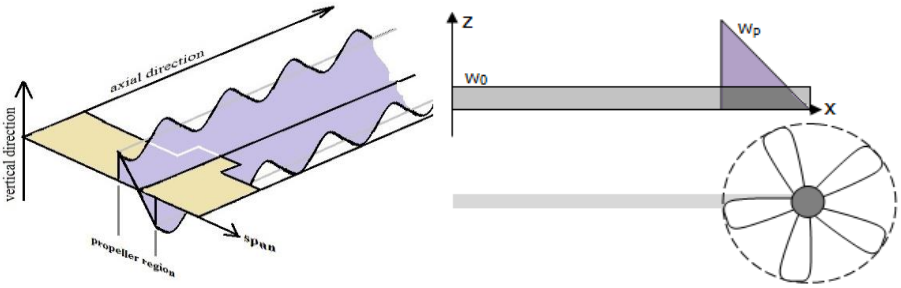

Figure 1: Propeller-axial (yellow) and vertical (purple) velocity contributions

The propeller axial effect and the constant span-wise advancing flow due to the forward flight form an advancing speed profile. Wagner's model considers the changes of the angle of attack ($\alpha_{\mathrm{AoA}} = \alpha + \dot{\xi} + (1/2 - a)\dot{\alpha}$) to formulate the dimensionless aerodynamic lift component as

$$l_a(x,\tau) = -\frac{2}{\mu}\phi(\tau)\alpha_{\mathrm{AoA}}(0) - \frac{2}{\mu}\int_0^\tau \phi(\tau-\tau_0)\dot{\alpha}_{\mathrm{AoA}}(\tau_0)\,d\tau_0 - \frac{1}{\mu}\left(\ddot{\xi} - a\ddot{\alpha} + \dot{\alpha}\right)$$
$$m_a(x,\tau) = -\frac{1}{r_\alpha^2}\left(\frac{1}{2}+a\right)l_a(x,\tau) + \frac{a}{r_\alpha^2\mu}\left(\ddot{\xi} - a\ddot{\alpha}\right) - \frac{1}{r_\alpha^2\mu}\left(\frac{1}{2}-a\right)\dot{\alpha} - \frac{1}{8}\frac{1}{r_\alpha^2\mu}\ddot{\alpha} \qquad (2)$$

Eq. (2) gives the Wagner's component for lift l_a and moment m_a in dimensionless form with $\mu = m/\pi\rho b^2$ being the mass parameter and a being the dimensionless distance between shear and chord centres. In the model presented, Wagner's function $\phi(\tau)$ is defined as Jones' exponential approximation [2, 3] for its simplicity of the recursive algorithm used. However, other forms of the approximation can be found in References [11, 12].

In the vertical direction, a linear gust profile is assumed, as shown by the purple area in Figure 1. Due to the harmonic nature of the propeller, a sinusoidal gust is assumed with 10% of the vertical gust effect as its variation amplitude. Thus, the total vertical gust w_G in the propeller covered area includes the pre-twist angle equivalent gust w_0, the propeller inflow contribution w_p and the sinusoidal gust variation at frequency k_p and magnitude w_i.

$$w_G(x,\tau) = w_0(x,\tau) + w_p(x,\tau) + |w_i(x)|\sin(k_p\tau - k_p(1+a)) \qquad (3)$$

In the rest of the wing span, only w_0 is present. The Küssner's function enables the modelling of aerofoil going through arbitrary gust field as successive step changes, and it defines lift generated on the wing.

$$l_g(x,\tau) = -\frac{2}{\mu}\int_0^\tau w_G(\tau_0)\frac{d\psi(\tau-\tau_0)}{d\tau}\,d\tau_0\,;\; m_g(x,\tau) = -\frac{1}{r_\alpha^2}\left(\frac{1}{2}+a\right)l_g(x,\tau) \qquad (4)$$

Here, the Küssner's function $\psi(\tau)$ is defined as approximated by Sears and Sparks [1]. Other forms of Küssner's function can be found in References [12].

2.3 Aeroelastic Model

A general matrix form of the governing equations can be obtained by combining the structural dynamics equations and the aerodynamic loadings and then by applying Galerkin's method. Indicating with **M**, **C** and **K** the mass, damping, and stiffness matrices, the following equation is obtained, where $\boldsymbol{u}$ and $\boldsymbol{F}$ are displacement and loading vectors, respectively

$$\mathbf{M}\ddot{\boldsymbol{u}} + \mathbf{C}\dot{\boldsymbol{u}} + \mathbf{K}\boldsymbol{u} = \boldsymbol{F}. \tag{5}$$

This system has been integrated using the Newmark-beta algorithm described below.

2.4 Recursive Algorithm

To overcome numerical inefficiency, a recursive algorithm has been used to store all the time history in the functions $X(\tau)$ and $Y(\tau)$, and simply update them once at each time step [12]. Taking the Wagner's function as an example to illustrate the algorithm, the lift l_a can be written as

$$\begin{aligned} l_a &= \frac{2}{\mu}\left\{\alpha_{\mathrm{AoA}}(0)\phi(\tau) + \int_0^\tau \dot{\alpha}_{\mathrm{AoA}}(\tau_0)\left[1 - A_1 e^{-b_1(\tau-\tau_0)} - A_2 e^{-b_2(\tau-\tau_0)}\right]d\tau_0\right\} \\ &= \frac{2}{\mu}\{\alpha_{\mathrm{AoA}}(0)\phi(\tau) + [\alpha_{\mathrm{AoA}}(\tau_0)]_\tau^0 - X(\tau) - Y(\tau)\}, \end{aligned} \tag{6}$$

where $X(\tau)$ and $Y(\tau)$ are written as

$$X(\tau) = \int_0^\tau \dot{\alpha}_{\mathrm{AoA}}(\tau_0)A_1 e^{-b_1(\tau-\tau_0)}d\tau_0;\ Y(\tau) = \int_0^\tau \dot{\alpha}_{\mathrm{AoA}}(\tau_0)A_2 e^{-b_2(\tau-\tau_0)}d\tau_0.$$

The functions $X(\tau)$ can then be expressed recursively as

$$\begin{aligned} X(\tau+\Delta\tau) &= e^{-b_1\Delta\tau}X(\tau) + A_1 e^{-b_1(\tau+\Delta\tau)}\int_\tau^{\tau+\Delta\tau}\dot{\alpha}_{\mathrm{AoA}}(\tau)e^{b_1\tau_0}\,d\tau_0 \\ &= e^{-b_1\Delta\tau}X(\tau) + A_1\frac{1-e^{-b_1\Delta\tau}}{b_1}\frac{\alpha_{\mathrm{AoA}}(\tau+\Delta\tau)-\alpha_{\mathrm{AoA}}(\tau)}{\Delta\tau} \end{aligned} \tag{7}$$

A similar formulation, like Eq. (7), applies to $Y(\tau+\Delta\tau)$. Therefore, instead of using a convolutional integral, lift l_a can be expressed based on its value from the previous iteration. With the recursive algorithm applied in Wagner's and Küssner's model, the aerodynamic loadings can be formulated at each iteration, and hence overcome the inefficiency of the convolutional integral.

2.5 Newmark-beta Method

As stated before, the system in Eq. (5) has been solved using the Newmark-beta algorithm to obtain the displacement vector $\boldsymbol{u}$**.** A key setting in this method is the β parameter that defines the velocity and acceleration assumptions in the integration [9]. Typically, β=1/4 (constant acceleration method) and β=1/6 (linear acceleration method) are the most commonly used, while in both settings γ=1/2 is kept for zero damping. The constant acceleration method assumes the acceleration unchanged during the time interval chosen and defines the velocity and displacement based on the data obtained at the previous step. In the linear acceleration method, the velocity and displacement are instead defined considering a linear variation of the acceleration during the time interval. These two methods are compared and the most efficient is selected to perform the analyses. Another important parameter in the time integration is the time step. Convergence analyses relating to it have been also performed and are discussed in later sections.

3 RESULTS AND DISCUSSION

3.1 Solver Validation

The aeroelastic model presented has been validated against results from a nonlinear beam system that was studied using a Runge-Kutta approach by Shams et al. [13]. As illustrated in Figure 2, the beam was initially disturbed in bending for 0.2m at the tip under its pre-flutter condition. In comparison with the present model, an agreement is shown in the bending and torsion displacements. For the same condition, frequency and damping are well reproduced but small discrepancies can be found in the maximum amplitude of the torsional oscillations. However, as the motions were initially excited by a bending displacement, modes coupling due to nonlinearity terms present in Shams' model, but not included here, contribute to the differences observed.

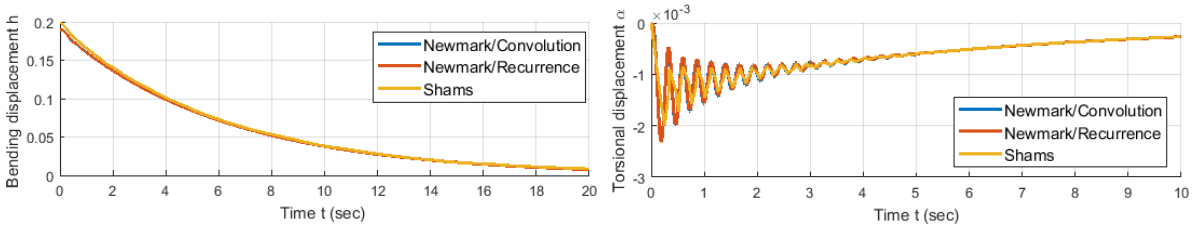

Figure 2: Tip dynamic response compared with Sham's results [13]

3.2 Case Study Parameters

For the case study presented, a wing-propeller system similar to Eurocopter X3 is considered and the main parameters are listed in Table 1. Note that the propeller sinusoidal gust is assumed with 10% of the vertical gust effect as its variation amplitude.

Mass per span length	35.9013 kg/m	Air density	1.225 kg/m^3
Moment of inertia per span length	0.2746 kg/m	Advancing speed	120 m/s
Bending stiffness (EI)	2.1413e+5 Nm^2		
Torsional stiffness (GJ)	2.4525e+5Nm^2	Propeller diameter	2 m
Chord length	0.5 m	Propeller mass	50 kg
Semi-wing span	2.0 m	Propeller location	Tip mounted
Shear & gravity centre offset	0 m	Propeller frequency	136.53 Hz
Shear centre and mid-chord offset	0 m	Advancing addition	8 m/s
Pretwist angle	2°	Max vertical induced	7 m/s

Table 1: Propeller-wing configuration details

Based on the parameters given, structural natural frequencies can be obtained as in Table 2.

1st Bending	2nd Bending	3rd Bending	4th Bending	1st Torsion
10.80 Hz	67.71 Hz	189.59 Hz	371.52 Hz	118.13 Hz

Table 2: Natural frequencies of bending and torsional modes

3.3 Case Study: Convergence

For a cantilever beam system, the number of modes considered in each coordinates affects the results accuracy. Also, the selection of other solver parameters and the time step for numerical integration determines the accuracy involved and the computational effort needed. For the present study, one steady-state vibration amplitude case is considered for convergence studies against the number of modes and the time step with two types of Newmark-beta algorithms.

Firstly, the steady-state amplitude is studied against the number of modes included, fixing the time-step to be 1/10 of the smallest period involved in the analysis. It is considered for the simulation to reach satisfactory convergence when the difference between two successive cases becomes less than 5%. Bending and torsion coordinates are studied separately taking a fixed number of modes in the coordinate not considered. Four different plots are shown in Figure 3 related to convergence studies performed with two different values of β used for the Newmark-beta algorithm. The red dashed curves show the numerical values of the steady-state amplitude (refer to RHS y-axis on the graphs) plotted against the number of modes considered. The blue curves show the percentage change comparing the solution at the point considered with the next data point obtained increasing number of modes included (refer to LHS y-axis on the graphs).

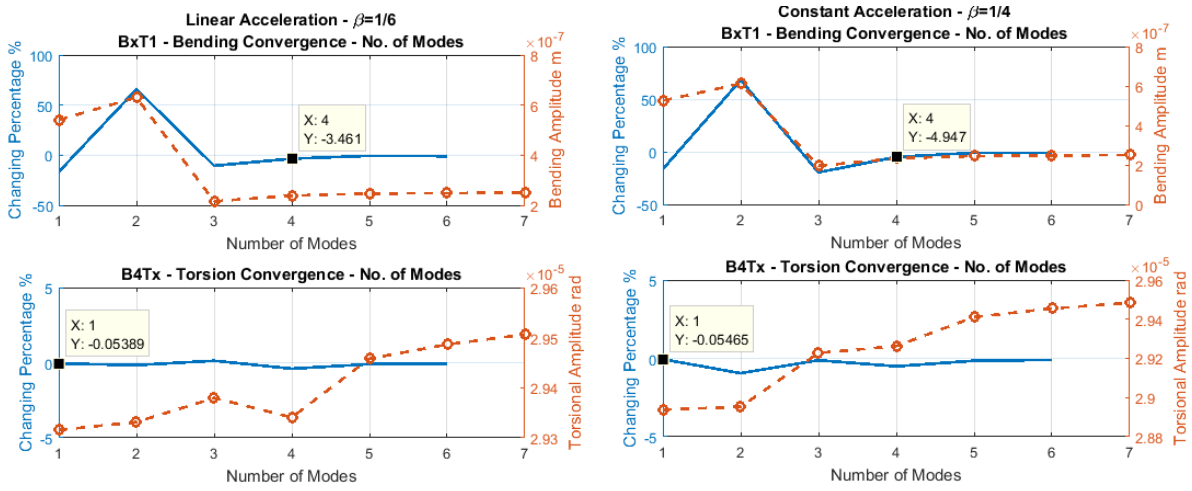

Figure 3: Convergence study for the number of modes needed

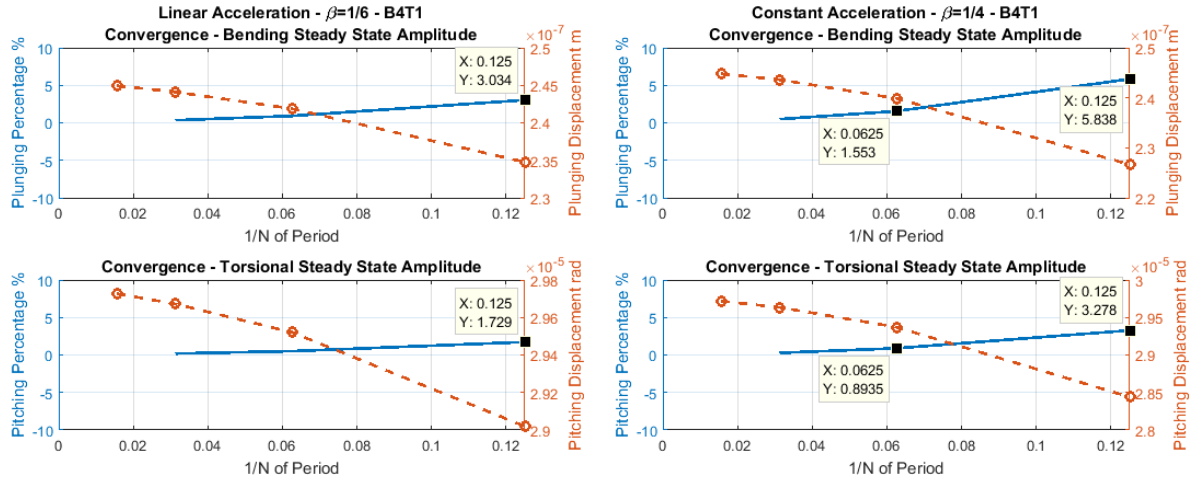

Figure 4: Convergence study for the time step

In torsional direction, the steady-state amplitude does not fluctuate significantly as more modes are included. A satisfactory convergence (within the 5%) can be found when include only the first mode. On the contrary, a drastic steady-state amplitude variation is observed in bending direction before the propeller frequency gets covered and a satisfactory level of convergence is reached with four modes. Therefore, four bending and one torsion modes are included for the case study analyses presented below. Furthermore, the effect of the β is also studied and illustrated in Figure 3. The linear acceleration approximation is found to give smaller percentage difference between iterations which makes it more efficient in this study.

Having decided the number of modes to include, a convergence study is carried out to study the impact of different time steps on the numerical results. Also in this case, two values for β parameter are explored. In Figure 4, numerical values of the steady-state amplitude show a smooth curve starting from the solution obtained with 1/8 of the smallest period involved. Comparing the two β values, the linear acceleration approximation is again proven to be more efficient, giving a smaller value variation for the same time step, and being able to meet satisfactory level of convergence with doubling of the time step size required for constant acceleration method. Therefore, the linear acceleration method with 1/8 of the smallest period is chosen in the study presented in the following.

3.4 Case Study: Results Comparison

In this section, results related to the wing response in the presence of propeller-wing interaction are shown. The wing is assumed to start from an unloaded initial condition and to be excited by the propeller stream, already in regime condition. This situation is not realistic during aircraft flight but it is considered to show the capability of the computational tool developed in modelling transient responses of the system with changes in the propeller regime. Furthermore, results given by the recursive algorithm and the convolutional integral are also compared in this section. For both cases, four bending and one torsion modes are considered with the iterative time step being 1/8 of the smallest period involved.

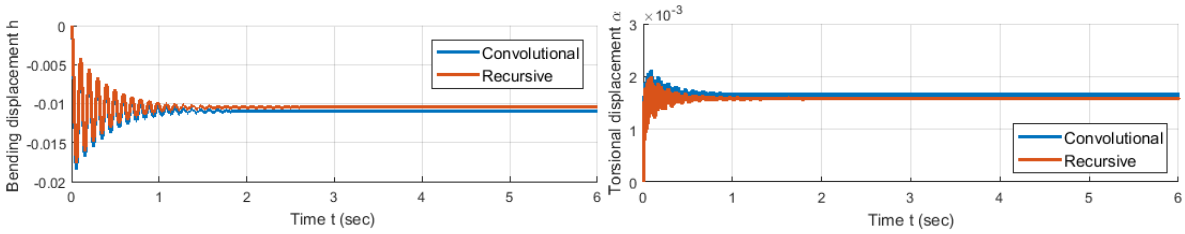

Figure 5: Time domain dynamic response at 75% span length for bending and torsion

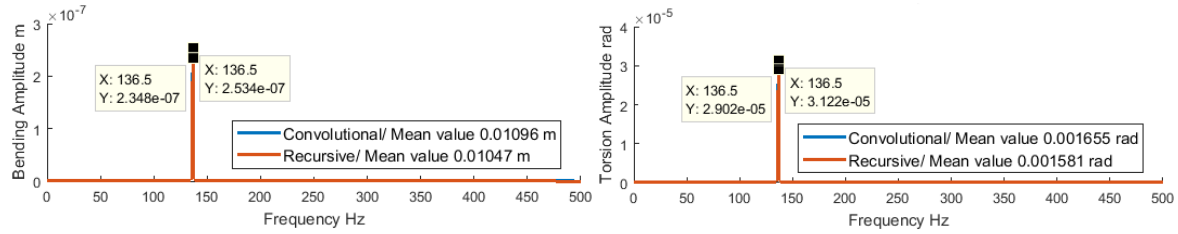

Figure 6: Steady state analysis in frequency domain

In Figure 5, dynamic responses related to the section located at 75% of wing span are illustrated over time of 6s for response. During the transient period, the dynamic behaviour is governed by the lowest wing's structural frequencies. As structural vibration dampens down and the structure reaches its steady state, the propeller frequency becomes more important in the response. Overall, the results obtained by both methods are very similar, and frequency and damping behaviour are very well aligned. Meanwhile, as shown in Figure 6, some differences in the steady-state amplitude and mean value are observed. Comparing the solutions from the two cases, in both the bending and the torsional directions, a difference within 5% is found for steady-state mean displacements and within 8% in the maximum steady-state amplitude. During the study, it was also found that these discrepancies approach zero as the time step decreases, even if this leads to higher computational effort. Considering the same problem settings, the computational time needed with the original form of convolutional integral took more than 1000 times longer than the case with the recursive algorithm in the analyses per-

formed. Furthermore, as the matrices size expands, the computation required with the convolutional integral increases exponentially. Therefore, the numerical tool with the recursive algorithm demonstrates to be much more efficient.

4 CONCLUSION

This paper presents efficient numerical methods for time-domain aeroelastic analysis for the purposes to provide accurate predictions of the system aeroelastic response. The present model is able to take into account torsional and flapping motions, pre-twist angle, stiffness variation, load distribution along the span and any arbitrary gust in in- and out-of-plane wing directions. The mathematical models used together with the numerical calculation performed are demonstrated. A detailed analysis of the solver for its convergence and accuracy is presented, as well as a case study for a Eurocopter X3-like propeller/wing configuration. In the case study, the recursive algorithm applied effectively improves the inefficiency of the convolutional integral and reduces drastically the computational effort needed.

REFERENCES

[1] W. R. Sears and B. O. Sparks, "On the reaction of an elastic wing to vertical gusts," *Journal of the Aeronautical Sciences,* vol. 9, no. 2, pp. 64-67, 1941.

[2] R. T. Jones, "Operational treatment of the nonuniform-lift theory in airplane dynamics," NACA Technical Notes No.667, 1938.

[3] R. T. Jones, "The unsteady lift of a wing of finite aspect ratio," NACA Technical Notes No.681, 1940.

[4] M. H. Kargarnovin and A. Mamandi, "Aeroelastic response for pure plunging motion of a typical section due to sharp edged gust , using Jones approximation aerodynamics," *World Academy of Science, Engineering and Technology,* vol. 36, pp. 154-161, 2007.

[5] S. Shams, H. Haddadpour, M. H. Sadr Lahidjani and M. Kheiri, "An analytical method in computational aeroelasticity based on Wagner function," in *25th International Congress of the Aeronautical Science,* Hamburg, Germany, 2006.

[6] P. Marzocca, L. Librescu and G. Chiocchia, "Aeroelastic response of 2-D lifting surfaces to gust and arbitrary explosive loading signatures," *International Journal of Impact Engineering,* vol. 25, no. 1, pp. 41-65, 2001.

[7] H. Wagner, "Über die Entstehung des dynamischen Auftriebes von Tragflügeln," *Zeitschrift für angewandte Mathematik and Mechanik,* vol. 5, no. 1, pp. 17-35, 1925.

[8] H. G. Küssner, "Zusammenfassender Bericht über den instationäran Auftrieb von Flügeln," *Luftfahrtforschung,* vol. 13, no. 12, pp. 410-424, 1935.

[9] N. Newmark, "A method of computation for structural dynamics," *Journal of the Engineering Mechanics Division,* vol. 85, no. 3, pp. 67-94, 1959.

[10] D. Hodges and G. Pierce, Introduction to structural dynamics and aeroelasticity, New York: Cambridge University Press, 2011.

[11] Y. Fung, An introduction to the theory of aeroelasticity, New York: Dover Publications Inc., 1955.

[12] J. Leishman, Principles of helicopter aerodyanmics, 2nd Edition, New York: Cambridge University Press, 2006.

[13] S. Shams, M. H. Sadr Lahidjani and H. Haddadpor, "Nonlinear aeroelastic response of slender wings based on Wagner function," *Thin-Walled Structures,* vol. 46, no. 11, pp. 1192-1203, 2008.